https://doi.org/10.15407/ujpe63.10.888

V.O. HRYN,[1] P.V. YEZHOV,[1] O.S. KUTSENKO,[2] T.M. SMIRNOVA [1]

[1] Institute of Physics, Nat. Acad. of Sci. of Ukraine
(46, Nauky Ave., Kyiv 03028, Ukraine; e-mail: vohryn@iop.kiev.ua)
[2] L.V. Pysarzhevskyi Institute of Physical Chemistry, Nat. Acad. of Sci. of Ukraine
(31, Nauky Ave., Kyiv 03028, Ukraine)

PROPERTIES OF PERIODIC STRUCTURES FORMED BY ORDERING SILVER NANOPARTICLES IN A POLYMER MATRIX USING THE HOLOGRAPHIC LITHOGRAPHY METHOD

The properties of one- and two-dimensional periodic structures formed by silver nanoparticles in polymer matrices have been studied. The thermo- or photostimulated synthesis of silver nanoparticles using the holographic lithography method occurs from a metal precursor previously distributed in the polymer matrix. The scheme of multibeam holographic recording is improved with the help of a liquid-crystal spatial light modulator. The mechanisms of periodic structure formation in the interference field, as well as the synthesis of silver nanoparticles, are considered. The relation between the parameters of nanoparticles and their spatial distribution, on the one hand, and the spectral properties of structures obtained in the polymer matrix, on the other hand, is studied.

K e y w o r d s: metal-polymer nanocomposites, silver clusters, silver nanoparticles, holographic lithography.

1. Introduction

Owing to the development of new materials for photonics, nanocomposites created on the basis of optically transparent matrices containing nanoparticles (NPs) of noble metals compose an important research field, since these materials demonstrate unique optical and electronic properties. Their specific properties mainly reveal themselves as the quantum and dielectric confinement effects, as well as the excitation of local surface plasmons in metal NPs [1–5]. Nanocomposites based on doped glass and polymers are most widely used in linear and nonlinear optics, laser physics, and optoelectronics [2–4].

Being compared with glass, polymers, besides a high variability of their structure and properties, are relatively cheap and quite easy to be manufactured. Polymer matrices can provide various modifications of their properties, such as the hydrophilicity or hydrophobicity, electrical insulating or conducting properties, as well as their mechanical rigidity or plasticity. Polymers are also effective stabilizers of metal NPs by preventing their aggregation [2]. Finally, the application of photopolymer compositions opens a possibility of producing submicronic periodic distributions of NPs in matrices using the simple one-stage holographic photopolymerization method [6, 7]. Nowadays, such nanocomposites are widely researched, and they are already used in various domains, e.g., as sensors [8–10], optical limiters [11] and filters [12, 13], for the optical encoding and storage of data [14, 15], for the amplification of spontaneous fluorescence and stimulated radiation emission in chaotic lasers by exciting plasmons [16, 17], and so forth.

The spectral position and the intensity of a plasmon resonance depend on the properties of separate metal NPs and their spatial arrangement, as well as on the properties of a dielectric matrix [11–14]. This dependence makes it possible to control the plasmonic properties of nanocomposites, which is implemented the most easily, if polymer matrices are applied. Despite that the researches in this direction have been carried out for a long time, the search for technologically simple and economically feasible methods aimed at creating structures with given properties still remains a challenging task.

One of the methods to control the plasmonic properties of nanocomposites is the structuring of such materials at the micronic and submicronic levels [15, 16]. Ordered structures with a submicronic period can be used as sensors [8], for the creation of optical memory and neural networks [17], as diffraction elements of a new type with an ultrahigh spectral dispersion [18, 19], and as resonators of waveguide lasers with a distributed feedback [20].

Two main procedures are applied to fabricate periodic structures "polymer-metal NPs" with the use of the holographic method. In the first case, NPs synthesized *ex situ* are introduced into a monomer mixture. Then the photopolymerization in the interference field is performed. A bulk structure is formed during the polymerization process as a result of the interdiffusion of the monomer and NPs. The emerged structure becomes stabilized due to the complete polymerization of the layer. This approach has a few shortcomings. First of all, metal NPs easily aggregate with one another in monomers. To obtain a homogeneous mixture, every NP has to be covered with a shell that should prevent it from the adhesion with other NPs, which makes the technology of element fabrication more complicated. Moreover, for recording the short-periodic structures, the radiation with a wavelength of 350–500 nm has to be used. But this is an interval, where the plasmon absorption bands of metals most widely used for producing NPs (Ag, Au, Cu) are located. As a result, the radiation recording a structure is absorbed that causes the structure nonuniformity in depth and correspondingly restricts the allowable NP concentration in the initial monomer mixture.

Earlier, we proposed an *in situ* method for the fabrication of periodic structures on the basis of silver NPs [21]. A solution of the metal precursor, from which the Ag nanoparticles are formed after the holographic recording, is introduced into the initial monomer mixture. Since the solutions, e.g., of gold or silver precursors absorb in the wavelength range $\lambda < 350$ nm, the holographic recording can be done in the whole visible range. A higher concentration of metal NPs can also be provided in comparison with the case where they are introduced into the prepolymer mixture.

In this work, we study the specific features in the formation, structure, and optical properties of one- (1D) and two-dimensional (2D) photonic crystals fabricated *in situ* and with the use of an original photopolymer composite. The mechanism of NP synthesis in the polymer matrix and the effect of nanocomposite structuring on the NP properties are also discussed.

2. Fabrication of One- and Two-Dimensional Periodic Structures

The fabrication stages of bulk periodic structures with the use of the holographic lithography method are illustrated in Fig. 1.

The initial composition was a mixture of bifunctional monomers: triethylene glycol dimethacrylate (TGM-3, 70 wt.%) and acryl-bis(propylene glycol)2,4-tolylene-diurethane (APGT, 30 wt.%). As a precursor of Ag nanoparticles, the solution of $AgNO_3$ in acetonitrile was used. The precursor was prepared by dissolving 0.1 g of an $AgNO_3$ powder in 1 ml of acetonitrile at room temperature. The obtained solution was introduced into the monomer mixture in an amount of 30 vol.% with respect to the monomer.

The "photoinitiator-sensitizer" system – a combination of Michler's ketone (MK, 1 wt.%) and camphorquinone (CQ, 5 wt.%) – provided the photosensitivity of composition in a spectral range of 440–500 nm. Polymer layers were formed as a result of

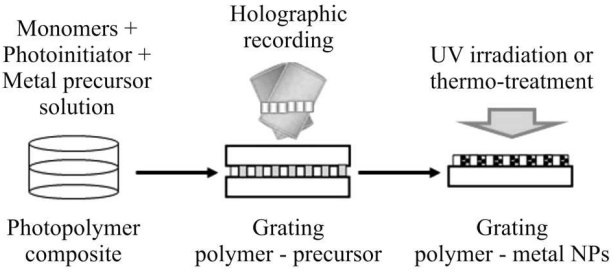

Fig. 1. Fabrication of bulk periodic structures

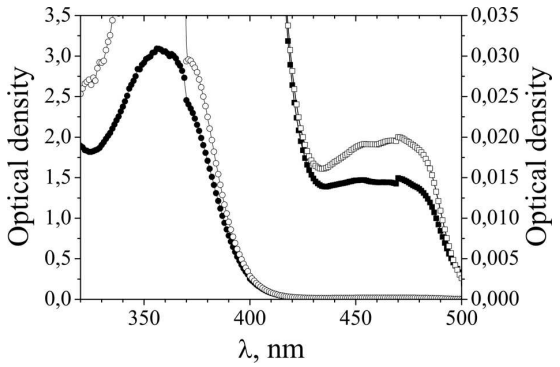

Fig. 2. Absorption spectra of the composition layer with acetonitrile before (open symbols) and after (solid symbols) the homogeneous photopolymerization at the irradiation with $\lambda > 400$ nm. The circles and the left ordinate axis correspond to the general spectrum, whereas the squares and the right ordinate axis to the absorption spectrum of camphorquinone

the radical photopolymerization of the composition under the action of radiation with a wavelength from the indicated spectral interval. The preparation of a composition is described in work [21] in detail. The reactivity of the composition held at a temperature of 10 °C for a month did not change.

Figure 2 demonstrate the absorption spectra of a composition layer with acetonitrile before and after the homogeneous photopolymerization by the irradiation with $\lambda > 400$ nm. The short-wave absorption band with a maximum at $\lambda \approx 358$ nm belongs to MK. The weak long-wave absorption band at $\lambda_{\max} \approx 450$ nm corresponds to the $n \to \pi$ transition in a CQ molecule. At the optimal CQ concentration, the absorption coefficient $K \leq 5$ cm^{-1} at the recording wavelength. Therefore, if the thickness of a recording layer $d \leq 100$ μm, the record practically takes place in the given field, which provides the grating uniformity over the layer thickness. In addition, as one can see from Fig. 2, in the course of the recording process, the sensitizer and the initiator undergo an irreversible phototransformation, which leads to the degradation of their absorption bands.

Layers for the holographic recording were fabricated by sandwiching a drop of initial liquid composition between two glass substrates, which were separated by calibrated spacers with a required thickness of 10–50 μm. Then the photosensitive layer was exposed to an interference pattern for recording a "polymer–metal precursor" holographic grating. After the holographic recording, the specimen surface was irradiated with uniform UV radiation in order to polymerize residual monomers in the region beyond the grating.

Silver NPs were mainly formed during an additional treatment of the polymer–precursor grating. For this purpose, after the recording, the substrate, which had been previously covered with an antiadhesive coating, was removed, and the grating was heated up at the temperature $T = 75$ °C for 1 h. The thermal treatment was repeated until the diffraction efficiency η reached a maximum value and saturated. At each stage, the grating parameters were monitored. A typical total time of the thermal treatment did not exceed 5 h. Silver could also be reduced by irradiating the gratings with UV radiation, but the reduction process was much slower in this case than at the thermal treatment.

3. Holographic Recording of 1D and 2D Structures

One-dimensional gratings were fabricated using the standard holographic recording scheme with two beams, which gives rise to the formation of transmission Bragg gratings. The spatial period of gratings depended on the convergence angle of the beams emitted by either an Ar^+ laser with the wavelength $\lambda = 488$ nm or a solid-state one MBL-III-473 with $\lambda = 471$ nm. The Ar^+ laser was used to record gratings with the spatial period in the range from 0.45 to 1 μm. Using the solid-state laser MBL-III-473, gratings with a maximum period of 3.5 μm were recorded. A He–Ne laser ($\lambda_t = 632.8$ nm) was used to monitor the process of grating formation. The intensities of laser beams transmitted through the grating, $I_{\rm tr}$, and diffracted on its structure, $I_{\rm dif}$, were monitored in the real-time mode with the help of a registration system. The diffraction efficiency η of the gratings was determined by the formula $\eta = I_{\rm dif}/(I_{\rm tr} + I_{\rm dif})$. In this case, the reflected or scattered radiation, as well as the absorption by the medium, was not taken into account.

For the gratings with the spatial periods in an interval of 0.4–1.0 μm, thicknesses of 10 μm or more were chosen, which, in accordance with the Cook–Klein parameter [22], allowed gratings of the Bragg type to be obtained. In this case, only the 0-th and 1-st diffraction orders were observed. The amplitude of the refractive index modulation, n_1, can be deter-

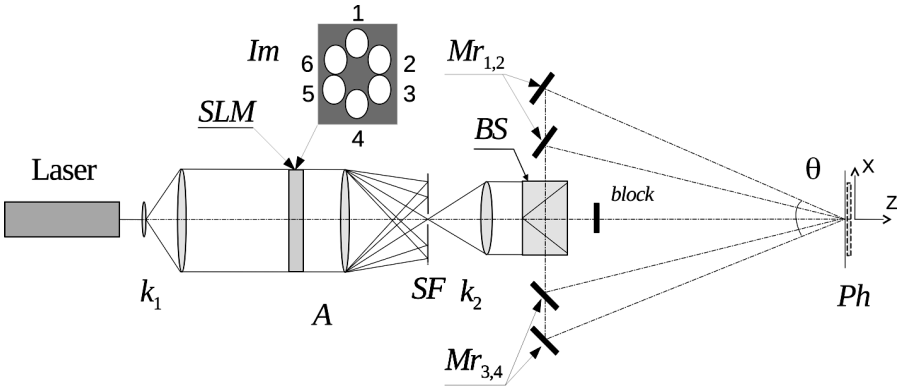

Fig. 3. Schematic diagram of the experimental installation for the six-beam recording of 2D structures: Laser – Ar^+ laser, k_1, k_2 – collimators, SLM – spatial light modulator with a given spatial phase distribution Im, SF – spatial filter, BS – prism system for the laser beam splitting, Mr_{1-6} – mirrors, θ – angle, and Ph – photosensitive medium

mined using the Kogelnik's formula [23]:

$$n_1 = \frac{\lambda_t \ \cos\theta_{\rm B} \ \arcsin\sqrt{\eta}}{\pi d},$$

where $\theta_{\rm B}$ is the Bragg angle in the medium, and d the grating thickness. To provide the Bragg diffraction for gratings with a period of 3.5 μm, their minimum thickness should be 50 μm.

When producing the 2D periodic structures with the help of the holographic lithography method [24], multibeam schemes are applied, as a rule. In order to obtain a required number of beams, prisms [25] or diffraction elements of various types are used, including spatial light modulators [26]. The types of elements and their arrangement were so selected to provide the required geometry of an interference pattern and, accordingly, the symmetry and size of the elementary cell in a photonic crystal [26–28].

Together with the variation in the number of beams and the angles between them, it is also of interest to control the phase relationships between the interfering beams [29], which provides an additional capability to affect the resulting intensity distribution in the recording plane. In work [30], we proposed a modification to the recording scheme, in which a spatial light modulator is applied to form the interference pattern. In Fig. 3, a schematic diagram of the six-beam recording scheme is shown, which enables hexagonal structures to be formed. Let us consider the work of this scheme.

A collimated beam of laser radiation passes through a spatial light modulator (SLM) of the transmission type. The SLM changes the phase distribution in such a way that there arise six beams with identical intensities I_{1-6} and given phases Φ_{1-6}. The notation Im in Fig. 3 marks an SLM plane, in which the beam geometry is shown. The areas of the common beam that are not involved are marked by the dark color. A spatial filter (SF) extracts the main SLM order and blocks the higher-order beams, starting from the $\pm$1-th orders. A system of prisms (BS) directs the beams to mirrors Mr_{1-6} (only mirrors Mr_{1-4} are shown), which form an interference pattern with a required period. The wave vector $\boldsymbol{k}_j$ of each j-th light wave (only I_{1-4} are shown) lies on the surface of cone with opening angle θ. It has the components $\boldsymbol{k}_{j,X}$, $\boldsymbol{k}_{j,Y}$, and $\boldsymbol{k}_{j,Z}$, where the Z-axis coincides with the cone axis. The interference field is formed in the 3D zone of the photosensitive medium (Ph) where the indicated waves mutually intersect. By varying the phase difference and the number of recording beams with the help of SLM and BS, we can form crystals with various symmetry types. It should be noted that, for some fixed phase differences between the interfering beams, there is no diffraction divergence along the Z-axis in the zone of their overlapping [29].

4. Properties of 1D Bulk Structures Polymer–Ag Nanoparticles

4.1. Formation mechanism of periodic structures polymer–Ag nanoparticles

The mechanism of grating formation is shown in Fig. 4. It was found that, in the course of photopoly-

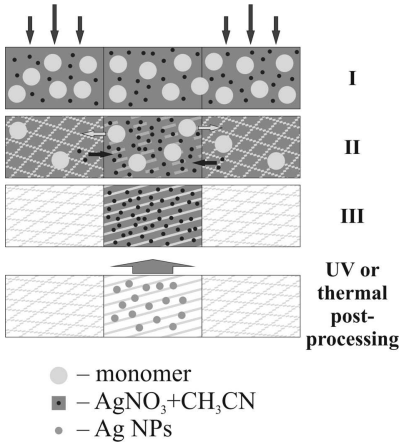

Fig. 4. Mechanism of grating formation

merization in a periodic light field, the main components – such as the monomer mixture and the metal precursor solution – participate in the irreversible photoinduced mass transfer between the illuminated and unilluminated regions of the interference pattern, which ensures the stability of the resulting structure. The precursor solution is displaced from the polymer network, which is formed and predominantly arranged in the grating grooves corresponding to high-intensity zones in the interference pattern. The precursor solution diffuses to the unilluminated zones. The complete composite polymerization provides the formation of a bulk structure including the periodically arranged regions consisting of the polymer and the polymer enriched with the metal precursor. The further thermal treatment of the specimen gives rise to the solvent evaporation and the formation of Ag nanoparticles predominately in the regions with the metal precursor.

Let us consider the mechanism of synthesis of Ag nanoparticles in more details. According to modern ideas [31], the process of silver NP synthesis in a monomer solution with a silver salt and a regenerator has the stage of Ag^+ reduction [$Ag^+ + e^- \to Ag_0$ (atom)], stage of Ag_x cluster formation [$xAg_0 \to Ag_x$ (NP)], and stage of cluster aggregation and NP size growth.

The mechanisms of Ag^+ photo- and thermal reduction and the influence of various composition components on them should be analyzed in a separate research. Now, we can propose a number of considerations that are consistent with the known data concerning the Ag^+ photoreduction. The photopolymerization of acrylic monomers using the MK photoinitiator is known for a long time [32]:

$$MK + MK \xrightarrow{h\nu} MK^*_{(+H)} + MK^*_{(-H)}. \quad (1)$$

The photochemical MK transformation leads to the formation of ketyl, $MK^*_{(+H)}$, and aminoalkyl, $MK^*_{(-H)}$, radicals. The latter is an active radical, which initiates the chain reaction of radical polymerization. In order to increase the aminoalkyl radical yield, benzophenone is traditionally used together with MK [33]. In our initiating system, CQ rather than benzophenone was applied as a polymerization sensitizer. The former not only absorbs at the recording wavelength, but, unlike the latter, has two, rather than one, carbonyl groups. This favors a larger yield of aminoalkyl radicals:

$$MK + CQ \xrightarrow{h\nu} MK^*_{(-H)} + CQ^*_{(+H)}. \quad (2)$$

As was noted above, the formed aminoalkyl radical $MK^*_{(-H)}$ initiates the polymerization reaction. In turn, the ketyl radical $CQ^*_{(+H)}$ can reduce Ag^+ according to the scheme:

$$Ag^+ + H^- + O^- \xrightarrow{h\nu} Ag^0 + H^+ + O^-.$$

At the acetonitrile evaporation, the condensation and crystallization of residual $AgNO_3$ take place, followed by the formation of a suspension of $AgNO_3$ nanoparticles in the matrix, as was in the case of silver halides in the gelatin matrix [34]. The further heating leads to the thermally stimulated reduction of monovalent silver, Ag(I), and the formation of silver nanoparticles. The analysis of the absorption spectra of the composite and the polymer layer obtained from it, which were registered before and after the heating, showed that the heating of specimens was accompanied by a decrease in the MK absorption band intensity, i.e. by the lowering of the MK concentration. This behavior gave us ground to assume that the $MK^*_{(+H)}$ and/or $CQ^*_{(+H)}$ radicals created in the thermally stimulated reactions (1) and (2) play a substantial role in the thermally stimulated silver reduction. In addition, the heating stimulates diffusion processes, which can also favor the reduction process activation.

4.2. Structure and spectral properties of polymer–Ag nanoparticle gratings

The spatial periodicity of the NP distribution in the polymer matrix was confirmed by analyzing a 1D grating with the help of a transmission electron microscope. The experimental technique was described in work [21] in detail. In a micrograph (Fig. 5), one can see that spherical NPs with an average diameter of about 5.25 nm (σ = 1.37 nm, panel *b*) form diffraction grating grooves.

The formation of NPs is also confirmed by changes in the extinction spectra of the gratings. In Fig. 6, the extinction spectra of 1D and 2D structures are shown. The bands with a maximum near 450 nm are characteristic of the excitation of local surface plasmons in the Ag nanoparticles. The band with a maximum at 360 nm belongs to the MK photoinitiator.

In Table, the values of the parameter n_1 obtained for gratings with various periods at a wavelength of 632.8 nm are quoted. A decrease of n_1 with the growth of the grating period is typical of media with the polymerization–diffusion mechanism of structure formation. In the case concerned, such a behavior is explained by a decrease in the modulation amplitude of the precursor solution concentration owing to an increase in the diffusion pathlength with the grating period. Note that the values obtained for n_1 are typical of holographic polymer nanocomposites. Hence, the formation of Ag nanoparticles gives rise to the spatial modulation of the dielectric constant of the nanocomposite and provides the formation of highly effective 1D structures.

The application of confocal scanning microscopy allowed us to study the mechanisms of formation and transformation of bulk holograms by visualizing the distribution profiles of the formation centers and measuring their local optical characteristics. A non-sinusoidal distribution of Ag nanoparticles that are formed at the heterogeneous polymerization in the interference field is depicted in Fig. 7 in the form of a local optical density profile measured for the light transmission through the grating. We also found grating components that luminesced at their excitation in various spectral intervals. The spatial distribution of the normalized photoluminescence intensity (PL/PL_{max}) was found to be in antiphase with respect to the absorption distribution of exciting light. In other words, the luminescence intensity of areas with low absorption (they corresponded to the intensity maxima of the interference field) exceeded that of the areas located at the interference field minima.

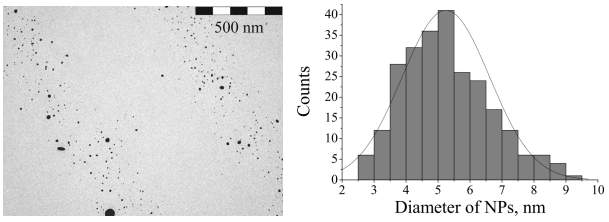

Fig. 5. TEM micrography of the structure (*a*) and a histogram of the nanoparticle size distribution (*b*)

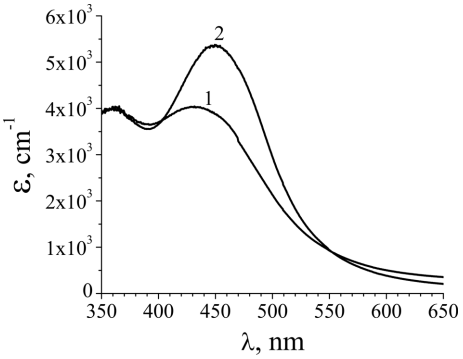

Fig. 6. Extinction spectra of 1D (*1*) and 2D (*2*) structures

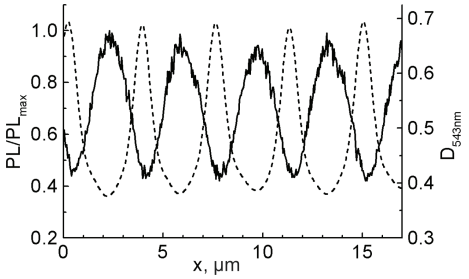

Fig. 7. Optical density (dashed curve) and normalized luminescence intensity (solid curve) profiles along the grating vector

Parameters of 1D structure

Λ, μm	d, μm	η, %	n_1
0.40	20	0.75	0.0135
0.95	20	0.87	0.0142
3.5	50	0.97	0.0056

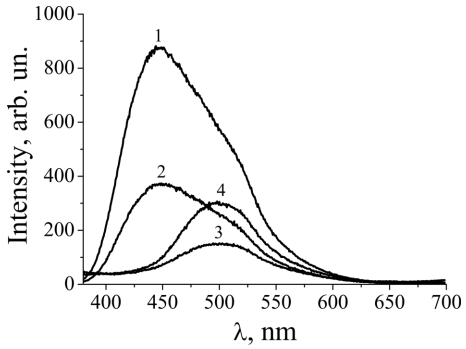

Fig. 8. Evolution of the integral grating luminescence spectrum under UV irradiation for 15 min (*1*), 1 h (*2*), 4 h (*3*), and 7 h (*4*)

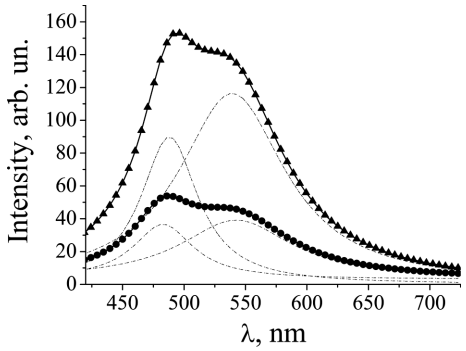

Fig. 9. Local grating luminescence spectra in illuminated (triangles) and unilluminated (circles) areas

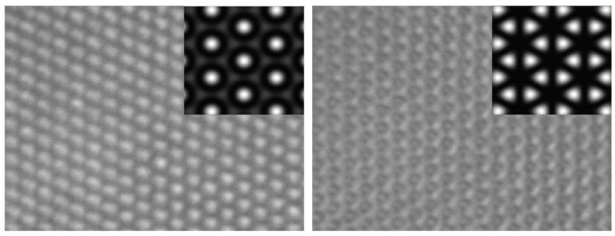

a *b*

Fig. 10. Crystal micrographs ($\Lambda_1 = 3.5$ μm) for $\Delta\Phi = 0$ (*a*) and 6π (*b*). The calculated intensity distributions in the interference patterns are shown in the insets

The examinations of the integral grating luminescence showed that the corresponding luminescence spectra are transformed in the course of post-processing (Fig. 8). After the recording, a broad band with a maximum at about 450 nm and most likely belonging to the MK is observed in the spectrum. The same band is observed in the spectrum of the polymer layer that contains MK and CQ, but does not contain Ag nanoparticles, because no metal precursor was added to the mixture. Under the influence of UV irradiation, the intensity of the MK band decreases, and there appears a new band with a maximum at about 500 nm. This band is absent from the luminescence spectrum of the polymer layer without NPs. Therefore, we may assume that it is emitted either by stable products that arise at the synthesis of Ag NPs or by silver clusters. It should be noted that there appear bands (not shown in the figure) in the spectrum in the course of post-processing, which correspond to intermediate products of the photo-induced NP synthesis and disappear after the processing is terminated.

The study of the spatial distribution of the grating luminescence spectrum showed that the spectral structure does not change at the grating areas corresponding to the maxima and minima of interference field. At the same time, the luminescence intensity in the illuminated areas substantially exceeds the intensity in the unilluminated areas (Fig. 9). Unlike the spectra shown in Fig. 8, in the case concerned, we observed a structured radiation band. In our opinion, in the spectra shown in Fig. 8, this structure can be hidden by the residual radiation emission of the products as a result of the synthesis process incompleteness.

The obtained results indicate to a higher quantum efficiency of luminescence in the hologram areas with low absorption and, accordingly, a low silver concentration. This fact proves that the indicated radiation cannot be emitted by Ag nanoparticles. It is known that silver clusters less than 1 nm in size and consisting of a few silver atoms, which we cannot observe in electron microscopic images, are able to luminesce. In work [21], it was shown that, unlike the relative NP concentration in the grating areas illuminated and unilluminated by the interference field (it is equal to unity), the relative modulation of the precursor concentration is equal to about 0.75. In other words, despite the presence of a metal precursor in both areas, NPs with sizes exceeding 1 nm are formed only in unilluminated areas. This may result from the rapid formation of a cross-linked polymer network in the illuminated areas, which prevents the formation of particles, whose sizes exceed 1 nm. The process is slowed down after the formation of small silver clusters, which may be responsible for the luminescence in the indicated areas. This assumption requires a further verification.

5. Properties of 2D Bulk Structures Polymer–Ag Nanoparticles

We also calculated the intensity distribution for an interference pattern formed by six beams. In the insets in Fig. 10, the intensity distributions for various hexagonal structures are shown. In the case corresponding to panel a, the total phase retradation between the beams (between the first and last ones) is equal to $\Delta\Phi = 0$. In the case corresponding to panel b, $\Delta\Phi = 6\pi$. The results correspond to structures described in work [29].

By applying the six-beam scheme, we obtained 2D photonic crystals, whose structures correspond to the calculated structures and are shown in the insets. The micrographs of the crystals are shown in Fig. 10. The images were obtained by focusing on the crystal surface.

A redistribution of zones corresponding to the dominant concentration of polymer and NPs was detected, when the phase shift between the recording beams was changed. As was indicated above, Ag nanoparticles are formed in the zones corresponding to the interference field minima, to which the $AgNO_3$ solution diffuses in the course of composition polymerization.

Having compared the field distributions and the structure pattern, we found that the light areas in the image correspond to the field maxima, i.e. areas, where the polymer concentration dominates, whereas the Ag nanoparticles become arranged in the dark areas. Thus, at the zero phase shift ($\Delta\Phi = 0$), the polymer zones form hexagons, being located at the corners and centers of hexagons. In the case of a nonzero phase shift between the recording beams (the case $\Delta\Phi = 6\pi$), the hexagons form areas that are enriched with Ag nanoparticles.

As one can see from the inset in Fig. 10, b, the polymer phase corresponding to the illuminated areas is also structured and forms hexagons around the areas, where Ag nanoparticles dominate (dark zones). Since Ag nanoparticles are formed immediately in the crystal, the size variation of the zones, in which they are formed, can affect the size and concentration of NPs. In works [35, 36], we showed that the structuring in the examined nanocomposite affects the dynamics of electron excitations in Ag nanoparticles and enhances the nonlinear nanocomposite response. The formulated issues are interesting from both scientific and practical viewpoints, and they will be a subject of our further research.

6. Conclusions

By studying the properties of bulk periodic structures composed of silver NPs in a polymer matrix, we obtained the following results.

Electron microscopy images and the profile of the local optical density of 1D structure indicate to a nonsinusoidal distribution of Ag nanoparticles formed at the inhomogeneous polymerization in the interference field. The periodic structure is formed by alternating a mere polymer phase and a polymer phase enriched with Ag NPs.

The spatial distribution of the luminescence intensity is in antiphase with respect to the local light absorption distribution in the structure, which indicates to a higher quantum luminescence efficiency in the areas with a low absorption and, accordingly, a low concentration of Ag nanoparticles. The most probable explanation for the spatial luminescence distribution is the formation of silver clusters with sizes smaller than 1 nm and possessing luminescence properties in the polymer areas corresponding to the interference maxima. The formation of Ag nanoparticles with sizes exceeding 1 nm may be hampered by the rapid formation of a dense cross-linked polymer network at the interference maxima, which restricts the diffusion-controlled reactions of NP synthesis.

The polymer nanocomposite provides a high contrast of 2D structures and unequivocally reflects a change in the intensity distribution of the interference pattern used for the holographic recording. The influence of symmetry and parameters of periodic structure, as well as the specific features of the polymer netwolrk formation, on the NP properties that are formed immediately in the structured composite, is a subject of our further research.

This work was supported by the grant of the Target Comprehensive Program of Fundamental Research of National Academy of Sciences of Ukraine "The Fundamental Problems of Creation of New Nanomaterials and Nanotechnologies" (Project 3/17-H). We also thank Dr. M. Stark and Dr. V. Chechik (University of York) for performing TEM measurements, and Dr. Sci. A. V. Veniaminov (SPb GUITMO) for his help in the studies of grating structural features.

1. U. Kreibig, M. Vollmer. *Optical Properties of Metal Clusters* (Springer, 1995) [ISBN: 978-3-642-08191-0].
2. L. Nicolais, G. Carotenuto. *Metal–Polymer Nanocomposites* (Wiley, 2004) [ISBN: 978-0-471-47131-8].
3. F. Gonela, P. Mazzoldi, H.S. Nalwa. *Handbook of Nanostructured Materials and Nanotechnology, Vol. 4* (Academic Press, 2000) [ISBN: 978-0-12-513760-7].
4. V.M. Shalaev. *Optical Properties of Nanostructured Random Media* (Springer, 2002) [ISBN: 978-3-540-42031-6].
5. I.M. Dmytruk. *Electron Processes in Nanostructures* (Kyiv, 2013) (in Ukrainian).
6. R.A. Vaia, C.L. Dennis, L.V. Natarajan, V.P. Tondiglia, D.W. Tomlin, T.J. Bunning. One-step, micrometer-scale organization of nano- and mesoparticles using holographic photopolymerization: a generic technique. *Adv. Mater.* **13**, 1570 (2001).
7. O.V. Sakhno, L.M. Goldenberg, J. Stumpe, T.N. Smirnova. Surface modified ZrO_2 and TiO_2 nanoparticles embedded in organic photopolymers for highly effective and UV-stable volume holograms. *Nanotechnology* **18**, 105704 (2007).
8. C. Hanisch, A. Kulkarni, V. Zaporojtchenko, F. Faupel. Polymer–metal nanocomposites with 2-dimensional Au nanoparticle arrays for sensoric applications. *J. Phys.: Conf. Ser.* **100**, 052043 (2008).
9. A. Sugunan, C. Thanachayanont, J. Dutta, J.G. Hilborn. Heavy-metal ion sensors using chitosan-capped gold nanoparticles. *Sci. Tech. Adv. Mater.* **6**, 335 (2005).
10. G. Sergeev, V. Zagorsky, M. Petrukhina, S. Zav'yalov, E. Grigor'ev, L. Trakhtenberg. Preliminary study of the interaction of metal nanoparticle-containing poly-p-xylylene films with ammonia. *Anal. Commun.* **34**, 113 (1997).
11. S. Porel, N. Venkatram, D.N. Rao, T.P. Radhakrishnan. In situ synthesis of metal nanoparticles in polymer matrix and optical limiting application. *J. Nanosci. Nanotechnol.* **7**, 1887 (2007).
12. Y. Dirix, C. Bastiaansen, W. Caseri, P. Smith. Oriented pearl-necklace arrays of metallic nanoparticles in polymers: a new route toward polarization-dependent color filters. *Adv. Mater.* **11**, 223 (1999).
13. I.E. Protsenko, O.A. Zaimidoroga, V.N. Samoilov. Heterogeneous medium as a filter of electromagnetic radiation. *J. Opt. A* **9**, 363 (2007).
14. H. Ditlbacher, J.R. Krenn, B. Lamprecht, A. Leitner, F.R. Aussenegg. Spectrally coded optical data storage by metal nanoparticles. *Opt. Lett.* **25**, 563 (2000).
15. B. Lamprecht, G. Schider, R.T. Lechner, H. Ditlbacher, J.R. Krenn, A. Leitner, F.R. Aussenegg. Metal nanoparticle gratings: influence of dipolar particle interaction on the plasmon resonance. *Phys. Rev. Lett.* **84**, 4721 (2000).
16. A.N. Ponyavina, S.M. Kachan. Plasmonic spectroscopy of 2D densely packed and layered metallic nanostructures. In *Polarimetric Detection, Characterization and Remote Sensing. NATO Science for Peace and Security Series C: Environmental Security* (Springer, 2011), p. 383.
17. P.N. Dyachenko, Yu.V. Miklyaev. One-dimensional photonic crystal based on nanocomposite of metal nanoparticles and dielectric. *Opt. Mem. Neural Networks* **16**, 198 (2007).
18. H. Ditlbacher, J.R. Krenn, G. Schider, A. Leitner, F.R. Aussenegg. Two-dimensional optics with surface plasmon polaritons. *Appl. Phys. Lett.* **81**, 1762 (2002).
19. V. Mikhailov, J. Elliott, G. Wurtz, P. Bayvel, A.V. Zayats. Dispersing light with surface plasmon polaritonic crystals. *Phys. Rev. Lett.* **99**, 083901 (2007).
20. J. Stehr, J. Grewett, F. Schindler, R. Sperling, G. von Plessen, U. Lemmer, J.M. Lupton, T.A. Klar, J. Feldmann, A.W. Holleitner, M. Forster, U. Scherf. A low threshold polymer laser based on metallic nanoparticle gratings. *Adv. Mater.* **15**, 1726 (2003).
21. T.N. Smirnova, L.M. Kokhtych, A.S. Kutsenko, O.V. Sakhno, J. Stumpe. Fabrication of periodic polymer/silver nanoparticles structures: *In situ* reduction of silver nanoparticles from precursor spatially distributed in polymer using holographic exposure. *Nanotechnology* **20**, 405301 (2009).
22. R.J. Collier, C.B. Burckhardt, L.H. Lin. *Optical Holography* (Academic Press, 1971).
23. H. Kogelnik. Coupled wave theory for thick hologram gratings. *Bell Syst. Tech. J.* **48**, 2909 (1969).
24. M. Campbell, D.N. Sharp, M.T. Harrison, R.G. Denning, A.J. Turberfield. Fabrication of photonic crystals for the visible spectrum by holographic lithography. *Nature* **404**, 53 (2000).
25. L. Wu, Y. Zhong, C.T. Chan, K.S. Wong, G.P. Wang. Fabrication of large area two- and three-dimensional polymer photonic crystals using single refracting prism holographic lithography. *Appl. Phys. Lett.* **86**, 241102 (2005).
26. S. Behera, J. Joseph. Design and realization of functional metamaterial basis structures through optical phase manipulation based interference lithography. *J. Opt.* **19**, 104079 (2017).
27. S. Indrišiūnas, B. Voisiat, M. Gedvilas, G. Račiukaitis. New opportunities for custom-shape patterning using polarization control in confocal laser beam interference setup. *J. Laser Appl.* **29**, 011501 (2017).
28. D. Lowell, J. Lutkenhaus, D. George, U. Philipose, B. Chen, Y. Lin. Simultaneous direct holographic fabrication of photonic cavity and graded photonic lattice with dual periodicity, dual basis, and dual symmetry. *Opt. Express* **25**, 14444 (2017).
29. M. Boguslawski, P. Rose, C. Denz. Increasing the structural variety of discrete nondiffracting wave fields. *Phys. Rev. A* **84**, 013832 (2011).
30. V.O. Hryn, P.V. Yezhov, T.N. Smirnova. Two-dimensional periodic structures recorded in nanocomposites by holographic method: features of formation, applications. In *Nanophysics, Nanomaterials, Interface Studies, and Applications. NANO 2016. Springer Proceedings in Physics, Vol. 195* (Springer, 2017), p. 293.

31. T.S. Kotsyuba, V.M. Granchak, I.I. Dilung. Influence of polarity of medium on formation of intermediates in photolysis of alkylaminobenzophenones in solutions. *Theor. Exp. Chem.* **33**, 26 (1997).
32. A. Ledwith. Photoinitiation by aromatic carbonyl compounds. *J. Oil Col. Chem. Assoc.* **59**, 157 (1975).
33. V.M. Granchak, T.S. Kotsuba, Z.F. Chemerskaya, I.I. Dilung. The role of oxygen in the origin of the synergistic effect of benzophenone and Michler's ketone in the initiation of radical photopolymerization. *Theor. Exp. Chem.* **31**, 91 (1995).
34. A.V. Yeltsov. *Photochemical Processes in Layers* (Leningrad, 1978) (in Russian).
35. T.N. Smirnova, P.V. Yezhov, S.A. Tikhomirov, O.V. Buganov, A.N. Ponyavina. Time-dependent absorption spectra of 1D, 2D plasmonic structures obtained by the ordering of Ag nanoparticles in polymer matrix. In *Nanophysics, Nanophotonics, Surface Studies, and Applications. Springer Proceedings in Physics, Vol. 183* (Springer, 2016), p. 131.
36. T.N. Smirnova, V.I. Rudenko, V.O. Hryn. Nonlinear optical properties of polymer nanocomposites with a random and periodic distribution of silver nanoparticles. In *Nanochemistry, Biotechnology, Nanomaterials, and Their Applications. NANO 2017. Springer Proceedings in Physics, Vol. 214* (Springer, 2018), p. 333.

Received 20.12.17.
Translated from Ukrainian by O.I. Voitenko

В.О. Гринь, П.В. Єжов, О.С. Куценко, Т.М. Смірнова

ВЛАСТИВОСТІ ПЕРІОДИЧНИХ СТРУКТУР, УТВОРЕНИХ ВПОРЯДКУВАННЯМ НАНОЧАСТИНОК СРІБЛА В ПОЛІМЕРНІЙ МАТРИЦІ МЕТОДОМ ГОЛОГРАФІЧНОЇ ЛІТОГРАФІЇ

Р е з ю м е

Досліджено властивості об'ємних одно- та двовимірних періодичних структур, утворених наночастинками срібла в полімерній матриці. Особливістю структур є те, що термоабо фотостимульований синтез наночастинок срібла відбувається в полімерній матриці з попередньо розподіленого методом голографічної літографії прекурсору металу. На основі просторового рідкокристалічного модулятора світла оптимізовано схему багатопучкового голографічного запису. Розглядаються механізми формування періодичних структур під дією інтерференційного поля і синтезу наночастинок срібла. Вивчається зв'язок спектральних властивостей отриманих структур з характеристиками наночастинок та їх просторовим розподілом в полімерній матриці.